Spark-induced Sparks as a Mechanism of Intracellular Calcium Alternans in Cardiac Myocytes

Robert Rovetti[1], **Xiaohua Cui**[2,3], **Alan Garfinkel**[3,4], **James N. Weiss**[4,5], and **Zhilin Qu**[4]

[1]Department of Mathematics, Loyola Marymount University, California 90045, USA

[2]Department of Physics, Beijing Normal University, Beijing 100875, P.R. China

[3]Department of Physiological Science, University of California, Los Angeles, California 90095, USA

[4]Department of Medicine (Cardiology), University of California, Los Angeles, California 90095, USA

[5]Department of Physiology, David Geffen School of Medicine, University of California, Los Angeles, California 90095, USA

Abstract

Rationale: Intracellular calcium (Ca) alternans has been widely studied in cardiac myocytes and tissue, yet the underlying mechanism remains controversial.

Objective: In this study, we used computational modeling and simulation to study how randomly occurring Ca sparks interact collectively to result in whole-cell Ca alternans.

Methods and Results: We developed a spatially-distributed intracellular Ca cycling model in which Ca release units (CRUs) are locally coupled by Ca diffusion throughout the myoplasm and sarcoplasmic reticulum (SR) network. Ca sparks occur randomly in the CRU network when periodically paced with a clamped voltage waveform, but Ca alternans develops as the pacing speeds up. Combining computational simulation with theoretical analysis, we show that Ca alternans emerges as a collective behavior of Ca sparks, determined by three critical properties of the CRU network from which Ca sparks arise: *randomness* (of Ca spark activation), *refractoriness* (of a CRU after a Ca spark), and *recruitment* (Ca sparks inducing Ca sparks in adjacent CRUs). We also show that the steep nonlinear relationship between fractional SR Ca release and SR Ca load arises naturally as a collective behavior of Ca sparks, and Ca alternans can occur even when SR Ca is held constant.

Conclusions: We present a general theory for the mechanisms of intracellular Ca alternans, which mechanistically links Ca sparks to whole-cell Ca alternans, and is applicable to Ca alternans in both physiological and pathophysiological conditions.

Keywords

Calcium sparks; Calcium alternans; Randomness; Refractoriness; Recruitment

Corresponding author: Zhilin Qu, PhD Department of Medicine (Cardiology) David Geffen School of Medicine at UCLA A2-237 CHS, 650 Charles E. Young Drive South Los Angeles, CA 90095 Tel: 310-794-6050 Fax: 310-206-9133 zqu@mednet.ucla.edu.

Introduction

Intracellular calcium (Ca) cycling plays a central role in cardiac excitation-contraction coupling [1, 2]. Ca alternans, a beat-to-beat alternation in intracellular Ca transient amplitude, is an important factor promoting T-wave alternans and pulsus alternans, markers conferring an increased risk of sudden cardiac death [3]. Although Ca alternans has been widely studied in cardiac myocytes [4-13], the underlying mechanism remains controversial. Eisner et al [4] were the first to propose that Ca alternans could be explained by a steep nonlinear dependence of sarcoplasmic reticulum (SR) Ca release upon the diastolic SR Ca load immediately preceding the release (a steep fractional release-load relationship). This mechanism requires that diastolic SR Ca load alternate concomitantly with SR Ca release. Subsequent experimental [6, 7, 9] and theoretical [9, 14, 15] studies have provided evidence supporting this mechanism. However, later experimental studies in rabbit ventricular myocytes by Picht et al [12] and in cat atrial myocytes by Hüser et al [13] showed that under some conditions, Ca alternans can be dissociated from the expected alternation in SR Ca content, raising questions about whether the mechanism proposed by Eisner et al is universally valid. Based on their observations, Picht et al suggested that refractoriness of ryanodine receptors (RyR) might play an important role in frequency-dependent Ca alternans.

In this study, we developed a spatially-distributed Ca cycling model to further investigate these issues. The model consists of a quasi-2D array of Ca release units (CRUs, also called couplons) which are coupled through Ca diffusion in the myoplasm and the SR network, from which Ca sparks, the elementary Ca release events of excitation-contraction coupling [16, 17], arise. According to current understanding, Ca sparks can be triggered by three mechanisms: 1) by opening of one or more L-type Ca channels (LCCs) in a CRU during an action potential, through a process called Ca-induced Ca release (CICR); 2) by spontaneous openings of RyRs, especially when SR Ca load is high, and 3) by Ca diffusing from nearby CRUs which have just released Ca from the SR, also through CICR. The first two mechanisms are well-documented experimentally, supporting the local control theory of Stern [18]. According to local control theory, the third mechanism of spark-induced sparks is generally assumed to be unimportant during normal excitation-contraction coupling. However, many experimental studies [17, 19] documenting the transitions from Ca spark to Ca wave indicate that spark-induced sparks become significant at some point as SR Ca load progressively increases. The exact point at which this occurs is not well-defined, but experiments by Parker et al [20] and Brum et al [21] have shown evidence of sparks triggering additional sparks, or sparks occurring sequentially, especially along the Z-line. Since both LCCs and RyRs open stochastically, Ca sparks tend to occur sparsely and randomly at low LCC open probability and/or under strong Ca buffering conditions [22, 23], but more regularly at higher LCC open probability and weak Ca buffering, e.g., for sparks evoked by action potentials in normal rabbit myocytes [24]. Finally, once a CRU releases Ca, it becomes refractory to further Ca release for a certain time period, i.e., there is a refractory period. Thus Ca sparks exhibit restitution, such that their amplitude depends on the time interval from the previous Ca spark [19, 25, 26].

To incorporate these general features into our model, we represented LCCs and RyRs using random-walk Markov models. Using computer simulation of our spatially-distributed Ca cycling model together with nonlinear dynamics analysis, we show how three generic CRU properties, including *randomness* (the stochastic nature of Ca sparks), *refractoriness*, and *recruitment* (the ability of one spark to recruit its neighboring CRUs to spark, or *spark-induced sparks*), interact synergistically to result in Ca alternans. Our simulations and theory agree with the experimental observations by Diaz et al [6, 7] that irregular, asynchronous Ca release is required for Ca alternans, with local Ca waves triggered during the large-release beat. However, we also show that a steep fractional release-load relationship emerges naturally as a collective behavior of the CRU network and Ca alternans can even occur when SR Ca content is held

constant. This agrees with the experimental observations by Picht et al [12] and Hüser et al [13] that alternans in diastolic SR Ca load is not required for Ca alternans.

Methods and Materials

Spatially-distributed Ca cycling model

We developed a quasi-2D spatially-distributed Ca cycling model (Fig.1), which includes a network SR (NSR) domain and a myoplasmic (Myo) domain coupled via SR Ca release and uptake. As illustrated in Fig.1A, this model comprises a CRU network coupled via Ca diffusion in each domain. Each CRU contains (Fig.1B): a junctional SR (jSR) which is diffusively connected to the NSR (J_{SR}), and a dyadic space (DS), which is diffusively connected to the myoplasm (J_{DS}). Extracellular Ca (J_{LCC}) enters the dyadic space through voltage-gated LCCs (5 channels per CRU), which open stochastically and are simulated by a simple Markov model (Fig.1C). Ca is released from the jSR (J_{RyR}) through its associated cluster of RyRs (100 channels per CRU) to the DS. The RyRs also open stochastically, and are simulated using a Markov model by Stern et al [27] (Fig.1D), in which activation and inactivation of RyRs are regulated by Ca in DS (with no regulation by SR luminal Ca). Ca is either extruded from the cell via the Na-Ca exchanger (J_{NCX}), or taken back up into the NSR via the SERCA pump (J_{up}). Since at the resting potential the Na-Ca exchanger always extrudes Ca, to maintain a stable Ca equilibrium state, we also added a background Ca current (J_b) to bring Ca into the myoplasmic domain. A network of 100×100 CRUs was used in this study. The differential equations and parameter values used in this study are detailed in Online Supplemental Data.

Computer simulation

We discretized the local NSR and the myoplasm domains of each CRU into 5×5 grids. Thus, a 100×100 CRU network was discretized into two coupled 500×500 grids. The differential equations were numerically simulated using an operator splitting method by advancing first the diffusion step and then the remaining reaction steps using a first-order forward Euler method with time step $\Delta t = 5$ μs. The stochastic transitions of LCC and RyR were updated asynchronously using an explicit method with a variable time step ($\Delta t = 5$ μs to 1 ms) adapted to the local Ca concentrations. The details of the numerical and simulation methods are presented in Online Supplemental Data.

Results

Steep relationship between SR Ca release and SR Ca load

A steep relationship between SR Ca release and SR Ca load (steep fractional release-load relationship), which plays an important role in regulating contractile force during normal excitation-contraction coupling, has been implicated in the genesis of Ca alternans, as described earlier. To explore the mechanism, we paced our CRU network model with a voltage clamp waveform to evoke Ca release from the SR. After achieving steady state, we recorded the whole-cell SR Ca content just before stimulation, and Ca depletion after stimulation (see inset of Fig.2A). By changing the amplitude of the background Ca current to alter the SR load, we obtained the relationship between SR Ca depletion and SR Ca load (Fig.2A, black symbols). The fractional release (Fig.2B) was small and insensitive to SR Ca content when SR load was low, but increased steeply between 600 μM and 700 μM, saturating at around 50%. For each SR load, we also calculated the total number of sparks (Fig.2C). The number of sparks increased slowly at low SR load, but increased steeply between 600 μM and 700 μM, beyond which the spark number saturated (at 10,000, the total number of CRUs in the system). To examine how fractional release is linked to sparks, we calculated the average whole-cell SR depletion <ΔCa> by summating the Ca depletion due to each individual spark, i.e.,

$$<\Delta Ca> = \sum_{i=1}^{N_{spark}} \left(Ca_{SR} - Ca_b^i \right) / N_{total} = (Ca_{SR} - <Ca_b>) \, N_{spark}/N_{total},$$

(1)

where Ca_{SR} is the luminal SR Ca content before each release, Ca_b^i is the minimum SR Ca content of the ith CRU after the depletion (with $<Ca_b> = \Sigma_{i=1}^{N_{spark}} Ca_b^i / N_{spark}$ being the average post-depletion content), N_{spark} is the number of sparks evoked, and N_{total} is the total number of CRUs. Using the spark data in Fig.2C and $<Ca_b> = 430$ μM, the predicted Ca depletion (open circles in Figs.2A) using Eq.1 agrees well with the direct measurements. Note that $<Ca_b> = 430$ μM is close to the depletion levels seen in individual sparks (see Figs.3 and 4, and online Fig.IV). Therefore, in our model in which Ca release by individual CRUs is not regulated by SR luminal Ca, a steep fractional release-load relationship nevertheless emerges as a collective behavior of the network, in proportion to the fraction of CRUs in the network generating sparks. In other words, a steep release-load relationship is not required as a property of individual CRUs in order for the CRU network, as a whole, to exhibit this behavior. The behavior arises because when SR and myoplasm reach equilibrium, higher SR Ca content translates to a higher mean Ca concentration in myoplasm and DS. At higher resting Ca in DS, a smaller increment in Ca is needed to induce opening of RyRs. Therefore, as Ca increases, the probability of Ca sparks triggered either by Ca influx through LCC openings or by Ca released from the neighboring CRUs also increases in a nonlinear fashion, as shown in Fig.2.

From random Ca sparks to whole-cell Ca alternans

When the CRU network model is paced periodically with a clamped voltage waveform at slow rates, the whole-cell Ca transient and diastolic SR Ca load are regular (Fig.3A). Although the summated Ca transient is regular, individual Ca sparks occur irregularly. In Fig.3B, we plot several traces of Ca from individual jSR spaces ("Ca blinks" [28], black), dyadic spaces (Ca sparks, red), and LCC Ca fluxes (blue) in arbitrarily selected CRUs. It can be seen that Ca sparks, blinks, and LCC openings occur more or less randomly. A spark may occur with or without LCC openings, and LCC openings in a CRU may or may not cause a Ca spark. Sparks occurring without companion LCC openings are sometimes induced by neighboring sparks (spark-induced sparks). Blinks of small amplitude can occur in the absence of sparks at a given location, since Ca release in a CRU drains Ca from neighboring CRUs via diffusion in the NSR. We calculated the numbers of CRUs with LCC openings, total sparks, LCC-triggered sparks (sparks with LCC openings) and recruited sparks (sparks without LCC openings), which are shown in online Fig.IA. In this case, about 70% of the CRUs release Ca on each beat, of which 70% are LCC-triggered sparks, and 30% are spark-induced sparks. Since Ca sparks occur randomly, the spatial distribution of myoplasmic Ca exhibits a random spatial pattern, which changes from beat to beat (Fig.3C), similar to the irregular pattern observed during action potential clamps in mouse ventricular myocytes [22], although different from rabbit ventricular myocytes [24] (see Discussion). In addition, CRUs tend to release Ca in clusters due to spark-induced sparks, resulting in spreading Ca waves (Fig.3D), which are sporadic and abort locally. Space-time plots (line-scan) exhibit random and patch-like patterns, resembling the experimental data by Diaz et al [6] (see online Fig.II).

As the pacing cycle length (PCL) decreases, whole-cell Ca alternans emerges. During alternans, both whole-cell myoplasmic Ca and SR Ca transients alternate in size from beat to beat (Fig.4A). The individual Ca sparks do not alternate but still occur randomly (Fig.4B), similar to the case of regular release (Fig.3B). However, the whole-cell spatial Ca pattern alternates from beat to beat (Fig.4B, see also the online video). Note that Ca sparks are sporadic and infrequent during the small Ca transients. During the large Ca transients, the sparks are still randomly distributed in space, but become more frequent. During alternans, the local waves

occur during the large Ca transient (Fig.4D) but rarely during the small Ca transient, in agreement with the observations of Diaz et al [7]. Also notice that the number of CRUs triggered by LCC openings only alternates slightly (online Fig.IB), indicating that many LCC openings during the small Ca beat do not successfully trigger Ca sparks. The recruitment rate (defined as the ratio of recruited sparks to LCC triggered sparks) alternates between 15% and 30% (online Fig.IC). In a time-space plot (line-scan), the alternating pattern (online Fig.III) resembles the experimental data from Diaz et al [7].

During both regular pacing and rapid pacing-induced alternans, the duration of Ca sparks varies from about 30 ms to >100 ms (online Fig.IV). The local SR Ca depletions (blinks) largely coincide with local Ca sparks, but the recovery of the local SR Ca content always exhibits a slow phase, reflecting the overall recovery of the global SR Ca content. In addition, the local SR Ca may deplete before (online Fig.IVD) or after (online Fig.IVE) the corresponding CRU spark. These results generally agree with the experimental observations by Zima et al [29], and are attributed to the diffusion of Ca within the SR network.

Ca alternans and the steep fractional release-load relationship

To test whether a steep fractional release-load relationship is required for Ca alternans, as proposed in previous studies [4, 14], we clamped the SR Ca to a constant value, and paced the system as in Fig.4. Ca alternans still occurred (Fig.5A), indicating that steep release-load relationship is not required. However, we could only induce Ca alternans when Ca was clamped at a high level corresponding to the steep region of the fractional SR Ca release curve (between 600 μM and 700 μM), and over a limited range of cycle lengths. If the SR Ca was clamped at a level either below or above this, alternans did not occur.

To further analyze how SR Ca release is related to SR load, we used a "ramped pacing" protocol similar to Picht et al [12]. We initially paced the model at the control PCL of 500 ms, at which Ca alternans was already present, and then gradually increased the PCL to 2000 ms, at which Ca alternans was absent. A plot of the SR depletion versus SR load (Fig.5B) resembles the data from the experiment by Picht et al [12] (online Fig.V). In particular, note that the diastolic SR Ca content during periodic beating in the absence of Ca altenans (see Fig.5B) is significantly lower than the SR diastolic Ca immediately preceding the small-release beat during stable alternans. However the amount of Ca release is greater during the periodic beating in the absence of Ca alternans, indicating that the SR Ca release does not completely rely on SR Ca content.

A dynamical mechanism of Ca alternans

In a recent theoretical study [30], we demonstrated a period-doubling bifurcation in an array of coupled randomly excitable elements subjected to periodic forcing and hypothesized that the same mechanism might be applicable to Ca alternans in cardiac myocytes (although no direct comparison was made). The three critical properties of the array required for this behavior included two properties assigned to the individual excitable elements (random activation and a refractory period), and one cooperative property between the elements (recruitment). Here we revisit the theory in terms of Ca sparks and Ca alternans and directly compare the general theory to the modeling results.

We assume that α is the probability of a primary Ca spark (Fig.6A), activated either spontaneously (due to high SR load or leakiness) or by opening of LCCs in the CRU; γ is the probability of a primary Ca spark recruiting a neighboring CRU to spark (secondary sparks); and β the probability that a CRU activated on the previous beat remains refractory during the present beat. If, on the kth beat, N_k out of N_0 total CRUs were activated, then on the $(k+1)^{th}$ beat, the number of CRUs available to be activated are $A_k = N_0 - \beta N_k$, since βN_k CRUs are still

in the refractory state. The number of primary sparks at the $(k+1)^{th}$ beat is then αA_k. The number of secondary sparks will be a fraction (f) of the remaining available (recovered) CRUs, i.e., $(1-\alpha)A_k f$. Therefore, the total number of activated CRUs during the $(k+1)^{th}$ beat is:

$$N_{k+1} = \alpha A_k + (1-\alpha) A_k f = (N_0 - \beta N_k)[\alpha + (1-\alpha) f] \qquad (2)$$

Eq.2 relates the number of Ca sparks in the present beat to the number of Ca sparks in the previous beat. What determines the fraction f? For an intuitive understanding, we show two schematic plots in Fig.6B for two beats in which CRUs have either mostly regained excitability (high recovery), or mostly remained refractory (low recovery). Since the spatial distribution of excitable and refractory CRUs is random in both cases, excitable CRUs are more isolated from each other in the case when most CRUs are refractory. This makes recruitment more difficult and leaves more potentially excitable CRUs unrecruited when the system is less recovered, and thus the recruitment rate is lower. Besides recovery, f also depends on primary spark rate α, recruitment probability γ, and the number of nearest neighbors. Using a mean-field approximation [30], we explicitly derived f as (see Online Supplemental Data):

$$f(\alpha,\beta,\gamma,N_k) = 1 - [1 - \alpha\gamma(1 - \beta N_k/N_0)]^n \qquad (3)$$

where n is the number of neighbors of a CRU. The recruitment rate, defined as the ratio of recruited sparks to primary sparks, i.e., $(1-\alpha)A_k f/\alpha A_k$, is then:

$$recruitment\ rate = (1-\alpha) f/\alpha \qquad (4)$$

The recruitment rate (Eq.4) for different α and γ is shown in Fig.6C along with the direct numerical results. Recruitment rate increases as γ increases, or as the number of recovered CRUs increases, but decreases as α increases.

Inserting Eq.3 into Eq.2, the steady state equilibrium of the system and its stability can be explicitly analyzed (see Online Supplemental Data). The stability of the steady state depends on α, β, and γ, and also on the function for f (and its slope). When the steady state becomes unstable, alternans occurs. Behaviors of Eq.2 are illustrated in the α−γ parameter space in Fig. 6D, with alternans occurring in the region above the line for each n (number of neighbors). In general, alternans occurs when α is intermediate (Fig.6E), γ is large, and β is large. Note that the large slope of the recruitment ratio curves shown in Fig.6C also occurs at intermediate α and large γ. Outside the alternans regime, a transient alternans due to initial condition can be observed, but quickly converges to the stable steady state (Fig.6F). However, alternans is persistent in the alternans regime (Fig.6G) where the steady state is unstable.

The parameters α, β, and γ in Eq.2 do not explicitly appear in the Ca cycling model, but can be linked to physiological parameters in the physiologically detailed Ca cycling model to gain mechanistic insights into Ca alternans, as illustrated by the examples below:

1) The parameter α is affected by factors such as the open probabilities of the LCC and RyR channels and the Ca content of the myoplasm and the SR. For example, decreasing LCC open probability is analogous to decreasing α. If the LCC open probability is high (thus α is high), based on the theoretical predictions shown in Figs.6D and E, then inhibiting the LCC current (thereby lowering α) should promote alternans, which indeed occurs in our spatially-distributed Ca cycling model (Fig.7A). This was also observed experimentally in voltage-clamped myocytes by partially blocking LCC [31, 32]. α can also be affected by extracellular Ca concentration $[Ca]_o$. Lower $[Ca]_o$ corresponds to smaller

α. Fig.7B shows that alternans occurs in the intermediate range of $[Ca]_o$ in our Ca cycling network model, agreeing with the theoretical prediction that alternans occurs in the intermediate range of α. This also agrees with the experimental observations that overloading the cell with extracellular Ca can either promote [33] or suppress [34] Ca alternans.

2) The probability *β* that a CRU remains refractory after a previous spark can be attributed to either intrinsic RyR channel properties or RyR regulation by SR luminal Ca, such as by calsequestrin binding to the RyR protein complex [35, 36]. Our theory predicts that alternans can occur only when β is very large, indicating that either prolonging the refractory period or shortening the stimulation period (which increases β) will promote alternans if α and γ are also properly chosen. For example, Schmidt et al [35] showed in mouse heart that overexpression of calsequestrin promoted pulsus alternans and Restrepo et al 37 showed in a modeling study that increasing calsequestrin concentration prolonged RyR refractoriness and promoted alternans, in agreement with our theoretical predictions. Fig.7C shows that, in our simulations using the spatially-distributed Ca cycling model, alternans is promoted by decreased PCL, consistent with the standard experimental method of inducing alternans by decreasing PCL.

3) The spatial cooperativity parameter γ, reflecting mainly the sensitivity of CICR, is affected by Ca level in the myoplasm, Ca diffusion rate, and the spacing between CRUs. For example, increasing CRU spacing makes recruitment less efficient (thus decreasing γ), which, based on our theory, suppresses alternans. This is demonstrated in the simulation results shown in Fig.7D. In their modeling study, Restrepo et al [37] showed that increasing the Ca diffusion rate (and thus increasing γ) promoted alternans, agreeing with our mean-field theory predictions. In addition, loading the cell with more Ca increases the sensitivity of RyRs to CICR, which enhances both the primary spark rate α and recruitment rate γ, thus promotes Ca alternans as $[Ca]_o$ increases from low to high (Fig.7B).

Discussion

In this study, we developed a spatially-distributed Ca cycling model to investigate how Ca sparks interact cooperatively to generate the steep fractional release-load relationship and Ca alternans. We show that Ca alternans emerges naturally as a result of three generic properties of the CRUs: *randomness*, *refractoriness*, and *recruitment*. Two of these three properties represent intrinsic CRU properties (random activation of Ca sparks and the refractory period of a CRU), whereas the third (recruitment, or spark-induced sparks) is governed by the spatial cooperativity between CRUs. In this Ca cycling model, Ca alternans does not causally rely on either regulation of RyR by SR luminal Ca, or a steep fractional release-load relationship, as proposed previously [4]. This is not to imply that the latter regulatory features do not exist or are unimportant, but merely to show that they are not formally required to produce Ca alternans when a generic mechanism of RyR refractoriness, coupled with randomness and recruitment, is present.

Randomness

A typical myocyte consists of 10,000-20,000 CRUs with each CRU containing 5-20 LCCs and 50-300 RyRs [1, 17, 38-40]. Since both LCC and RyR open randomly, Ca sparks are also naturally random, but their degree of randomness depends on the open probability of LCC and RyR. For example, if one assumes that only one LCC is needed to trigger a spark, and if a CRU has 10 LCCs, each with a low open probability of 0.05, the probability that none of the LCCs will open on a given depolarization is $(1-0.05)^{10}=0.6$, so that the probability of a spark is only 0.4. However, for the same CRU in which the open probability of LCC is 0.5, the probability that none of the LCC will open is reduced to $(1-0.5)^{10}=0.001$, so that a Ca spark will occur on virtually every beat. Equivalently, if the LCC open probability is high, but the probability of

an LCC opening activating the RyRs is low, the Ca spark probability will also decrease. In our mean-field theory, α is the parameter describing the random excitability of the LCC and RyR channels. In the extreme case, when α=1, all CRUs will fire as primary sparks at each beat, no recruitment can occur and thus alternans cannot develop. As illustrated in Fig.6, randomness is also necessary for the steep nonlinear recruitment function *f*. If the recovered CRUs were not randomly distributed, it would be hard to image how such a nonlinear recruitment function *f* can emerge. In fact, alternans in the experiments by Diaz and colleagues [6, 7, 32] was induced by either reducing LCC open probability (with LCC blockers or mildly depolarized voltage clamp pulses), or coupling fidelity (with RyR blockers or acidosis to reduce RyR open probability). In addition, they observed in their confocal imaging studies that asynchronous Ca release was needed for alternans. Their studies provide direct experimental support for our theoretical argument that randomness is necessary for alternans. Our prediction that random spark activation plays a key role in alternans might seem incompatible with the observation that when rabbit ventricular myocytes are paced with an action potential clamp at rates too slow to induce alternans, sparks occur regularly from the same sites[24]. However, we predict that when the rate is increased sufficiently to induce Ca alternans, this regular spark appearance will deteriorate and become asynchronous, due to the reduction in coupling fidelity as the rapid heart rate impinges upon RyR refractoriness. This will be an important experimental test of the theory.

It has been shown experimentally that Ca release becomes asynchronous in diseased heart [41, 42], which may be caused by a lower primary spark rate (α) resulting from remodeling processes, such as T-tubule disruption [43, 44], altered excitation-contraction coupling, and altered cooperativity between RyRs within the same CRU. Lowering α enhances not only randomness, but also enhances recruitment (because more CRUs are available to be recruited), which may be one of the predisposing causes of alternans in ischemia [45], heart failure [46], and catecholaminergic polymorphic ventricular tachycardia [47].

Refractoriness

After RyRs in a CRU open and release Ca, they inactivate and require time to recover excitability. RyRs are the pore-forming proteins mediating SR Ca release, but co-assemble with a variety of accessory proteins which regulate their open probability and sensitivity to myoplasmic free Ca. Although the precise molecular basis of CRU refractoriness remains controversial, several nonexclusive mechanisms have been proposed: 1) Intrinsic RyR refractory period, as in the model proposed by Stern et al (Fig. 1D). In the simplest mechanism, RyRs undergo conformational changes between different states, similar to other ligand-gated channels, one of which is a refractory state. 2) Direct regulation of RyR open probability by SR luminal Ca. In this mechanism, RyRs are activated by increased myoplasmic free Ca, but their sensitivity is also coregulated by a Ca-binding site in the C terminus of RyR, which senses SR luminal free Ca [48]. 3) Indirect regulation of RyR open probability by SR luminal Ca. In this mechanism, RyRs are activated by increased myoplasmic free Ca, but the sensitivity is coregulated by calsequestrin, through its interaction with accessory proteins such as triadin and junctin in the RyR protein complex [49].

In terms of providing the refractoriness required in our analysis, any one of these three molecular mechanisms of RyR refractoriness is sufficient to account for alternans, whether SR luminal Ca regulation is absent (mechanism 1) or present (mechanisms 2 and 3). Although refractoriness is necessary for alternans in our theory, it is not sufficient without the other two factors (randomness and recruitment). Its role in alternans can be understood as follows (see also Figs.6B and C). Immediately prior to the beat with a large Ca transient, most of the CRUs are recovered (since they did not spark on the prior beat with a small Ca transient). Thus, available CRUs are densely distributed, such that their probability of recruiting secondary

sparks is high (large f in Eq.2). Immediately afterwards, however, most CRUs will be refractory, since they were just activated. Thus, on the next beat following a large Ca transient, few CRUs are available and they will be sparsely distributed, and recruitment of secondary sparks is therefore low (small f in Eq.2).

In agreement with our theoretical argument, increasing RyR refractoriness by transgenic overexpression of calsequestrin was shown in both experiments [35] and simulations [37] to promote alternans. On the other hand, Ca alternans was also reported to be enhanced in a transgenic mouse model of catecholaminergic polymorphic ventricular tachycardia, in which RyR refractoriness was decreased [50]. It will be interesting to explore further whether specific combinations of randomness, refractoriness and recruitment can concomitantly promote both Ca alternans and Ca waves.

Recruitment

Recruitment, i.e., the efficiency of spark-induced sparks, is determined by spatial cooperativity between CRUs. It is mediated by Ca diffusion and is sensitive to a variety of factors, including the Ca concentrations in the myoplasm and SR, the SR Ca uptake and leak rates, Ca buffering, and the spacing between adjacent CRUs. The process of spark-induced sparks, combined with randomness and refractoriness, is crucial for the nonlinearity (recruitment function f in Eq.2) required for alternans. For example, as shown in online Fig.I, during steady state (PCL=1400 ms), the recruited sparks accounted for 30% of the total sparks (corresponding to recruitment rate 40%). During alternans (PCL=500 ms), the recruitment rate was around 30% on the large beat, but dropped to 15% on the small beat. Spark-induced sparks are also the basis of myoplasmic Ca waves due to CICR [19, 51], and therefore naturally link Ca waves to Ca alternans, as observed in experiments [5-7]. Our simulations show that reducing CRU spacing increases recruitment rate, and thus promotes alternans. This may be one of the predisposing causes of alternans in heart failure, in which remodeling has been shown to decrease CRU spacing [52]. Whether spark-induced sparks occur under normal conditions is unclear, but they are promoted by conditions of Ca overload (increased extracellular Ca or fast pacing), increased RyR sensitivity to SR or myoplasmic Ca, decreased CRU distance, etc. These conditions are known to be present in disease states [52, 53], consistent with the observation that Ca alternans and waves are promoted by heart failure and ischemia.

Steep nonlinear fractional Ca release-load relationship

A steep nonlinear release-load relationship is a fundamental property of cardiac excitation-contraction coupling, and plays an important role in the physiological regulation of the whole-cell Ca transient amplitude, and hence contractile force, in response to changes in heart rate and autonomic tone which alter the SR Ca load. Both myoplasmic and luminal SR Ca regulation of RyRs have been suggested as possible sources for the steep nonlinear relationship [54]. Here we show that SR luminal Ca regulation of RyR is not strictly necessary for the steep release-load relationship and Ca alternans. The underlying source of the steep release-load relationship is a dual increase in both SR Ca and myoplasmic Ca level. The increase of myoplasmic Ca increases the open probability of the RyR and thus increases the Ca spark probability of a CRU. In addition, as myoplasmic Ca increases, the probability of spark-induced sparks also increases. These two factors cause the number of sparks to increase steeply and nonlinearly as the SR load increases, resulting in a steep nonlinear release-load relationship. Although the occurrence of Ca alternans is always accompanied by a steep fractional release-load relationship as observed in experimental studies [4, 6, 7, 11], a causal relation between the steep fractional release-load relationship and Ca alternans may not exist. In other words, both the steep fractional release-load relationship and alternans may be the result of enhanced CICR and spark recruitment, instead of one causing the other. On the other hand, although our model does not include SR luminal Ca regulation of RyR, we do not mean to imply that this feature is not

important, only that in a minimal CRU network, it is not an absolute requirement for either a steep release-load relationship or Ca alternans. In fact, experimental [35, 36, 49, 55] and modeling [37, 53] studies directly support luminal SR Ca regulation of RyR as playing important roles in Ca release and Ca alternans. However, it is more difficult to explain the dissociation of SR Ca load and release during Ca alternans as observed by Picht et al [12], if release is tightly regulated by luminal SR Ca load under all conditions. It is intriguing to speculate that luminal SR Ca regulations may have evolved as a refinement to an already present property of the CRU network, to provide robustness and/or a greater dynamic performance range.

Limitations

In our study, we have focused on the minimum properties of a CRU network required to produce Ca alternans. Several limitations need to be addressed in future studies. 1) A real myocyte is a three-dimensional system which contains a complex and heterogeneous CRU network coupled with a complex T-tubule network. 2) Only one of the three molecular mechanisms of refractoriness was studied in our Ca cycling model. 3) Many molecular signaling pathways regulate LCCs, RyRs, and SERCA pump. These molecular and sub-cellular factors undoubtedly play important roles in the genesis of Ca alternans. In addition, how intracellular Ca couples with membrane voltage to result in repolarization alternans and how the Ca alternans maintains synchronized in multi-cell tissue need to be investigated in future studies. Despite these limitations, our model and theory can explain the key experimental observations and provide a unifying general theory linking the steep fractional release-load relationship, Ca alternans and Ca waves in cardiac myocytes.

Novelty and Significance

What is known?

- Pulsus alternans and T-wave alternans are associated with cardiac arrhythmias and sudden death, and calcium alternans has been assumed to be one type of cellular alternans responsible for T-wave alternans and pulsus alternans of the heart.

- Calcium alternans tends to occur under conditions of calcium overload and fast heart rates in normal cells, and is exacerbated under diseased conditions such as heart failure and ischemia.

What new information does this article contribute?

- A computer model that simulates spatially-distributed Ca sparks and whole-cell Ca alternans.

- A novel mechanism of Ca alternans which links whole-cell Ca alternans to the properties of Ca sparks.

The mechanisms of calcium alternans are not well understood, and remain controversial. Using computer simulation and theoretical analysis, we developed a novel theory of calcium alternans which mechanistically links random, locally interacting calcium sparks to a stable whole-cell calcium alternans. We show that Ca alternans is a collective behavior of calcium sparks, driven by the synergistic interactions of three key properties of the calcium release units (CRUs): refractoriness of the CRUs, random activation of CRUs, and sparks inducing neighboring CRUs to spark. Through these three properties, one can link various molecular factors, such as calsequestrin regulation of the ryanodine receptors, and structural factors, such as the inter-CRU distance, to whole-cell alternans, providing a unified mechanistic understanding of calcium alternans due to seemingly unrelated causes.

Supplementary Material

Refer to Web version on PubMed Central for supplementary material.

Acknowledgments

Non-standard Abbreviations and Acronyms

Ca	calcium
SR	sarcoplasmic reticulum
RyR	ryanodine receptor
CRU	calcium release unit
LCC	L-type calcium channel
CICR	calcium-induced calcium release
NSR	network sarcoplasmic reticulum
jSR	junctional sarcoplasmic reticulum
DS	dyadic space
PCL	pacing cycle length

References

1. Bers DM. Calcium cycling and signaling in cardiac myocytes. Annu Rev Physiol 2008;70:23–49. [PubMed: 17988210]

2. ter Keurs HEDJ, Boyden PA. Calcium and arrhythmogenesis. Physiol Rev 2007;87:457–506. [PubMed: 17429038]

3. Weiss JN, Karma A, Shiferaw Y, Chen PS, Garfinkel A, Qu Z. From pulsus to pulseless: the saga of cardiac alternans. Circ Res 2006;98:1244–1253. [PubMed: 16728670]

4. Eisner DA, Choi HS, Diaz ME, O'Neill SC, Trafford AW. Integrative analysis of calcium cycling in cardiac muscle. Circ Res 2000;87:1087–1094. [PubMed: 11110764]

5. Blatter LA, Kockskamper J, Sheehan KA, Zima AV, Huser J, Lipsius SL. Local calcium gradients during excitation-contraction coupling and alternans in atrial myocytes. J Physiol 2003;546:19–31. [PubMed: 12509476]

6. Diaz ME, Eisner DA, O'Neill SC. Depressed ryanodine receptor activity increases variability and duration of the systolic Ca^{2+} transient in rat ventricular myocytes. Circ Res 2002;91:585–593. [PubMed: 12364386]

7. Diaz ME, O'Neill SC, Eisner DA. Sarcoplasmic reticulum calcium content fluctuation is the key to cardiac alternans. Circ Res 2004;94:650–656. [PubMed: 14752033]

8. Aistrup GL, Kelly JE, Kapur S, Kowalczyk M, Sysman-Wolpin I, Kadish AH, Wasserstrom JA. Pacing-induced heterogeneities in intracellular Ca^{2+} signaling, cardiac alternans, and ventricular arrhythmias in intact rat heart. Circ Res 2006;99:e65–73. [PubMed: 16960102]

9. Xie LH, Sato D, Garfinkel A, Qu Z, Weiss JN. Intracellular Ca alternans: coordinated regulation by sarcoplasmic reticulum release, uptake, and leak. Biophys J 2008;95:3100–3110. [PubMed: 18539635]

10. Gaeta SA, Bub G, Abbott GW, Christini DJ. Dynamical mechanism for subcellular alternans in cardiac myocytes. Circ Res 2009;105:335–342. [PubMed: 19628792]

11. Belevych AE, Terentyev D, Viatchenko-Karpinski S, Terentyeva R, Sridhar A, Nishijima Y, Wilson LD, Cardounel AJ, Laurita KR, Carnes CA, Billman GE, Gyorke S. Redox modification of ryanodine receptors underlies calcium alternans in a canine model of sudden cardiac death. Cardiovasc Res 2009;84:387–395. [PubMed: 19617226]

12. Picht E, DeSantiago J, Blatter LA, Bers DM. Cardiac alternans do not rely on diastolic sarcoplasmic reticulum calcium content fluctuations. Circ Res 2006;99:740–748. [PubMed: 16946134]

13. Huser J, Wang YG, Sheehan KA, Cifuentes F, Lipsius SL, Blatter LA. Functional coupling between glycolysis and excitation-contraction coupling underlies alternans in cat heart cells. J Physiol 2000;524(Pt 3):795–806. [PubMed: 10790159]

14. Shiferaw Y, Watanabe MA, Garfinkel A, Weiss JN, Karma A. Model of intracellular calcium cycling in ventricular myocytes. Biophys J 2003;85:3666–3686. [PubMed: 14645059]

15. Tao T, O'Neill SC, Diaz ME, Li YT, Eisner DA, Zhang H. Alternans of cardiac calcium cycling in a cluster of ryanodine receptors: a simulation study. Am J Physiol Heart Circ Physiol 2008;295:H598–609. [PubMed: 18515647]

16. Cheng H, Lederer WJ, Cannell MB. Calcium sparks: elementary events underlying excitation-contraction coupling in heart muscle. Science 1993;262:740–744. [PubMed: 8235594]

17. Cheng H, Lederer WJ. Calcium Sparks. Physiol Rev 2008;88:1491–1545. [PubMed: 18923188]

18. Stern MD. Theory of excitation-contraction coupling in cardiac muscle. Biophys J 1992;63:497–517. [PubMed: 1330031]

19. Cheng H, Lederer MR, Lederer WJ, Cannell MB. Calcium sparks and $[Ca^{2+}]_i$ waves in cardiac myocytes. Am J Physiol 1996;270:C148–159. [PubMed: 8772440]

20. Parker I, Zang WJ, Wier WG. Ca^{2+} sparks involving multiple Ca^{2+} release sites along Z-lines in rat heart cells. J Physiol 1996;497(Pt 1):31–38. [PubMed: 8951709]

21. Brum G, Gonzalez A, Rengifo J, Shirokova N, Rios E. Fast imaging in two dimensions resolves extensive sources of Ca^{2+} sparks in frog skeletal muscle. J Physiol 2000;528:419–433. [PubMed: 11060121]

22. Bridge JH, Ershler PR, Cannell MB. Properties of Ca^{2+} sparks evoked by action potentials in mouse ventricular myocytes. J Physiol 1999;518(Pt 2):469–478. [PubMed: 10381593]

23. Wang SQ, Song LS, Lakatta EG, Cheng H. Ca^{2+} signalling between single L-type Ca^{2+} channels and ryanodine receptors in heart cells. Nature 2001;410:592–596. [PubMed: 11279498]

24. Inoue M, Bridge JH. Ca^{2+} sparks in rabbit ventricular myocytes evoked by action potentials: involvement of clusters of L-type Ca^{2+} channels. Circ Res 2003;92:532–538. [PubMed: 12609971]

25. Sobie EA, Song LS, Lederer WJ. Local recovery of Ca^{2+} release in rat ventricular myocytes. J Physiol 2005;565:441–447. [PubMed: 15817631]

26. Sobie EA, Song LS, Lederer WJ. Restitution of Ca^{2+} release and vulnerability to arrhythmias. J Cardiovasc Electrophysiol 2006;17(Suppl 1):S64–S70. [PubMed: 16686684]

27. Stern MD, Song LS, Cheng H, Sham JS, Yang HT, Boheler KR, Rios E. Local control models of cardiac excitation-contraction coupling. A possible role for allosteric interactions between ryanodine receptors. J Gen Physiol 1999;113:469–489. [PubMed: 10051521]

28. Brochet DX, Yang D, Di Maio A, Lederer WJ, Franzini-Armstrong C, Cheng H. Ca^{2+} blinks: rapid nanoscopic store calcium signaling. Proc Natl Acad Sci U S A 2005;102:3099–3104. [PubMed: 15710901]

29. Zima AV, Picht E, Bers DM, Blatter LA. Termination of cardiac Ca^{2+} sparks: role of intra-SR $[Ca^{2+}]$, release flux, and intra-SR Ca^{2+} diffusion. Circ Res 2008;103:e105–115. [PubMed: 18787194]

30. Cui X, Rovetti RJ, Yang L, Garfinkel A, Weiss JN, Qu Z. Period-doubling bifurcation in an array of coupled stochastically excitable elements subjected to global periodic forcing. Phys Rev Lett 2009;103:044102–044104. [PubMed: 19659359]

31. Luzza F, Oreto G. Verapamil-induced electrical and cycle length alternans during supraventricular tachycardia: what is the mechanism? J Cardiovasc Electrophysiol 2003;14:323–324. [PubMed: 12716120]

32. Li Y, Diaz ME, Eisner DA, O'Neill S. The effects of membrane potential, SR Ca^{2+} content and RyR responsiveness on systolic Ca^{2+} alternans in rat ventricular myocytes. J Physiol 2009;587:1283–1292. [PubMed: 19153161]

33. Saitoh H, Bailey JC, Surawicz B. Action potential duration alternans in dog Purkinje and ventricular muscle fibers: further evidence in support of two different mechanisms. Circulation 1989;80:1421–1431. [PubMed: 2553299]

34. Dumitrescu C, Narayan P, Efimov IR, Cheng Y, Radin MJ, McCune SA, Altschuld RA. Mechanical alternans and restitution in failing SHHF rat left ventricles. Am J Physiol Heart Circ Physiol 2002;282:H1320–1326. [PubMed: 11893567]

35. Schmidt AG, Kadambi VJ, Ball N, Sato Y, Walsh RA, Kranias EG, Hoit BD. Cardiac-specific overexpression of calsequestrin results in left ventricular hypertrophy, depressed force-frequency relation and pulsus alternans in vivo. J Mol Cell Cardiol 2000;32:1735–1744. [PubMed: 10966834]

36. Terentyev D, Viatchenko-Karpinski S, Valdivia HH, Escobar AL, Gyorke S. Luminal Ca^{2+} controls termination and refractory behavior of Ca^{2+}-induced Ca^{2+} release in cardiac myocytes. Circ Res 2002;91:414–420. [PubMed: 12215490]

37. Restrepo JG, Weiss JN, Karma A. Calsequestrin-mediated mechanism for cellular calcium transient alternans. Biophys J 2008;95:3767–3789. [PubMed: 18676655]

38. Soeller C, Crossman D, Gilbert R, Cannell MB. Analysis of ryanodine receptor clusters in rat and human cardiac myocytes. Proc Natl Acad Sci U S A 2007;104:14958–14963. [PubMed: 17848521]

39. Chen-Izu Y, McCulle SL, Ward CW, Soeller C, Allen BM, Rabang C, Cannell MB, Balke CW, Izu LT. Three-dimensional distribution of ryanodine receptor clusters in cardiac myocytes. Biophys J 2006;91:1–13. [PubMed: 16603500]

40. Franzini-Armstrong C, Protasi F, Ramesh V. Shape, size, and distribution of Ca^{2+} release units and couplons in skeletal and cardiac muscles. Biophys J 1999;77:1528–1539. [PubMed: 10465763]

41. Litwin SE, Zhang D, Bridge JH. Dyssynchronous Ca^{2+} sparks in myocytes from infarcted hearts. Circ Res 2000;87:1040–1047. [PubMed: 11090550]

42. Gomez AM, Guatimosim S, Dilly KW, Vassort G, Lederer WJ. Heart failure after myocardial infarction: altered excitation-contraction coupling. Circulation 2001;104:688–693. [PubMed: 11489776]

43. Louch WE, Mork HK, Sexton J, Stromme TA, Laake P, Sjaastad I, Sejersted OM. T-tubule disorganization and reduced synchrony of Ca^{2+} release in murine cardiomyocytes following myocardial infarction. J Physiol 2006;574:519–533. [PubMed: 16709642]

44. Brette F, Orchard C. T-tubule function in mammalian cardiac myocytes. Circ Res 2003;92:1182–1192. [PubMed: 12805236]

45. Qian YW, Clusin WT, Lin SF, Han J, Sung RJ. Spatial heterogeneity of calcium transient alternans during the early phase of myocardial ischemia in the blood-perfused rabbit heart. Circulation 2001;104:2082–2087. [PubMed: 11673350]

46. Wilson LD, Jeyaraj D, Wan X, Hoeker GS, Said TH, Gittinger M, Laurita KR, Rosenbaum DS. Heart failure enhances susceptibility to arrhythmogenic cardiac alternans. Heart Rhythm 2009;6:251–259. [PubMed: 19187920]

47. Lehnart SE, Terrenoire C, Reiken S, Wehrens XHT, Song L-S, Tillman EJ, Mancarella S, Coromilas J, Lederer WJ, Kass RS, Marks AR. Stabilization of cardiac ryanodine receptor prevents intracellular calcium leak and arrhythmias. Proc Natl Acad Sci U S A 2006;103:7906–7910. [PubMed: 16672364]

48. Jiang D, Xiao B, Yang D, Wang R, Choi P, Zhang L, Cheng H, Chen SR. RyR2 mutations linked to ventricular tachycardia and sudden death reduce the threshold for store-overload-induced Ca^{2+} release (SOICR). Proc Natl Acad Sci U S A 2004;101:13062–13067. [PubMed: 15322274]

49. Gyorke I, Hester N, Jones LR, Gyorke S. The role of calsequestrin, triadin, and junctin in conferring cardiac ryanodine receptor responsiveness to luminal calcium. Biophys J 2004;86:2121–2128. [PubMed: 15041652]

50. Lehnart SE, Terrenoire C, Reiken S, Wehrens XH, Song LS, Tillman EJ, Mancarella S, Coromilas J, Lederer WJ, Kass RS, Marks AR. Stabilization of cardiac ryanodine receptor prevents intracellular calcium leak and arrhythmias. Proc Natl Acad Sci U S A 2006;103:7906–7910. [PubMed: 16672364]

51. Keizer J, Smith GD, Ponce-Dawson S, Pearson JE. Saltatory propagation of Ca^{2+} waves by Ca^{2+} sparks. Biophys J 1998;75:595–600. [PubMed: 9675162]

52. Chen-Izu Y, Ward CW, Stark W Jr. Banyasz T, Sumandea MP, Balke CW, Izu LT, Wehrens XH. Phosphorylation of RyR2 and shortening of RyR2 cluster spacing in spontaneously hypertensive rat with heart failure. Am J Physiol Heart Circ Physiol 2007;293:H2409–2417. [PubMed: 17630346]

53. Shannon TR, Wang F, Bers DM. Regulation of cardiac sarcoplasmic reticulum Ca release by luminal [Ca] and altered gating assessed with a mathematical model. Biophys J 2005;89:4096–4110. [PubMed: 16169970]

54. Shannon TR, Ginsburg KS, Bers DM. Potentiation of fractional sarcoplasmic reticulum calcium release by total and free intra-sarcoplasmic reticulum calcium concentration. Biophys J 2000;78:334–343. [PubMed: 10620297]

55. Terentyev D, Kubalova Z, Valle G, Nori A, Vedamoorthyrao S, Terentyeva R, Viatchenko-Karpinski S, Bers DM, Williams SC, Volpe P, Gyorke S. Modulation of SR Ca release by luminal Ca and calsequestrin in cardiac myocytes: effects of CASQ2 mutations linked to sudden cardiac death. Biophys J 2008;95:2037–2048. [PubMed: 18469084]
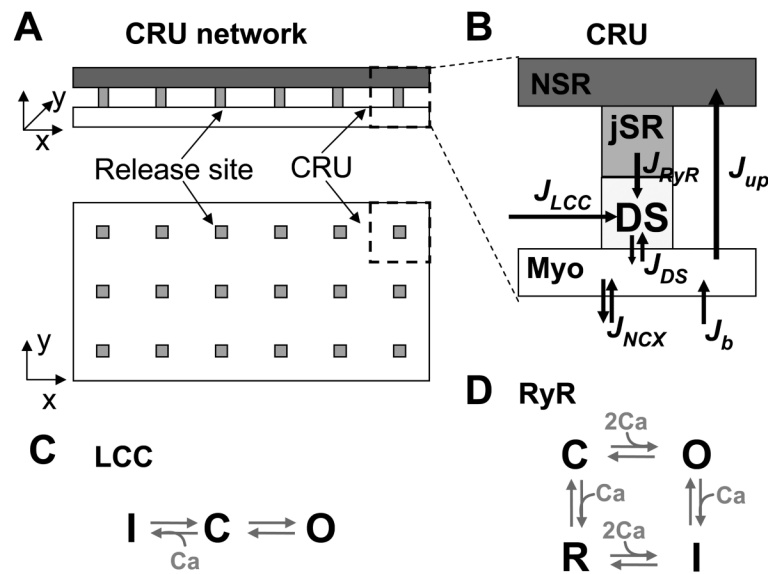
Figure 1. The spatially-distributed Ca cycling model
A. Schematic plots (side view and top view) of a coupled CRU network. **B**. A detailed illustration of a CRU. **C**. A simplified Markov model of the LCC. "O" is the open state and "I" and "C" are the closed states. The LCC is activated by voltage and inactivated by voltage and Ca (as indicated by "Ca" in the graph) in the dyadic space. **D**. The Markov model of the RyR from Stern et al [27]. "O" is the open state, "I", "R", and "C" are the closed states. RyR is activated and inactivated by Ca (as indicated by "Ca" in the graph) in the dyadic space.
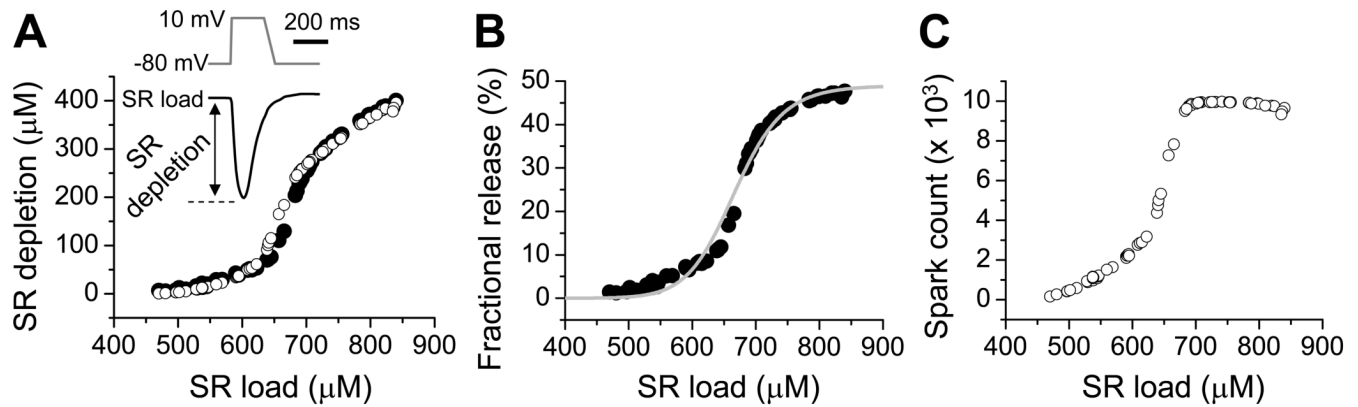
Figure 2. Steep fractional release-load relationship

A. SR Ca depletion versus SR Ca load measured in simulation (filled circles) and transformed using Eq.1 with $\langle Ca_b \rangle$=430 μM (open circles). Inset shows the voltage clamp wave form (upper) and the SR Ca trace (lower) illustrating the measurement of depletion versus load. SR Ca load was altered by changing the background Ca current (J_b) in the model (see Methods). **B**. Fractional Ca release versus SR Ca load. The fractional SR release was calculated from A using SR depletion divided by SR load. The gray line is the best fit with the Hill function:

$$\frac{0.49^*[Ca_{SR}]^{17.5}}{667^{17.5}+[Ca_{SR}]^{17.5}}$$

. **C.** Spark count versus SR Ca load in the corresponding simulations in A. In simulation, a spark is defined as occurring when the Ca concentration in the dyadic space surges above 10 μM.
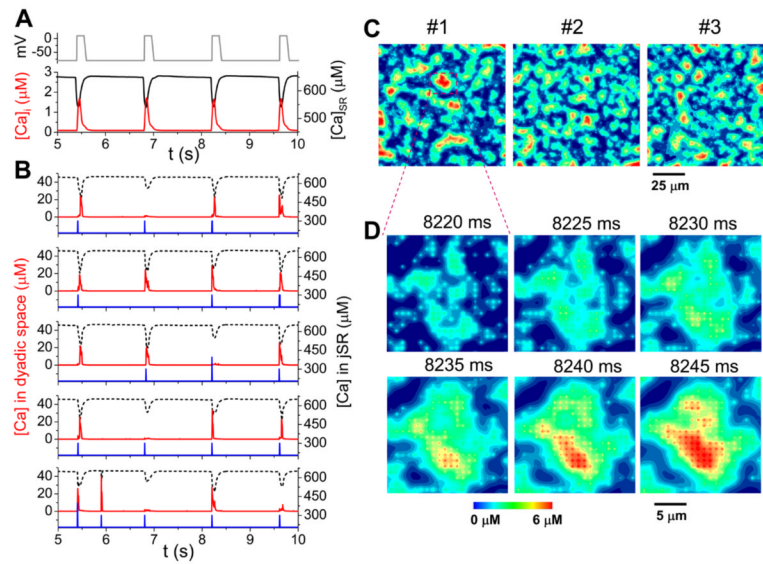
Figure 3. Ca transient in the Ca cycling model at slow pacing
A. Clamped voltage (top), whole-cell SR Ca concentration (black), and whole-cell myoplasm Ca concentration (red) versus time for PCL=1.4 s. **B**. Ca traces from jSR (black dashed) and dyadic space (red) at different spatial locations for the same simulation shown in A. The blue line in each panel shows the Ca fluxes through the LCCs in the corresponding CRUs. **C**. Snapshots of myoplasmic Ca spatial distribution taken at the moment of the Ca transient peaks for three consecutive beats. **D**. Ca snapshots from a small region (dashed box in beat #1 in panel C) show wave-like spread of Ca release.
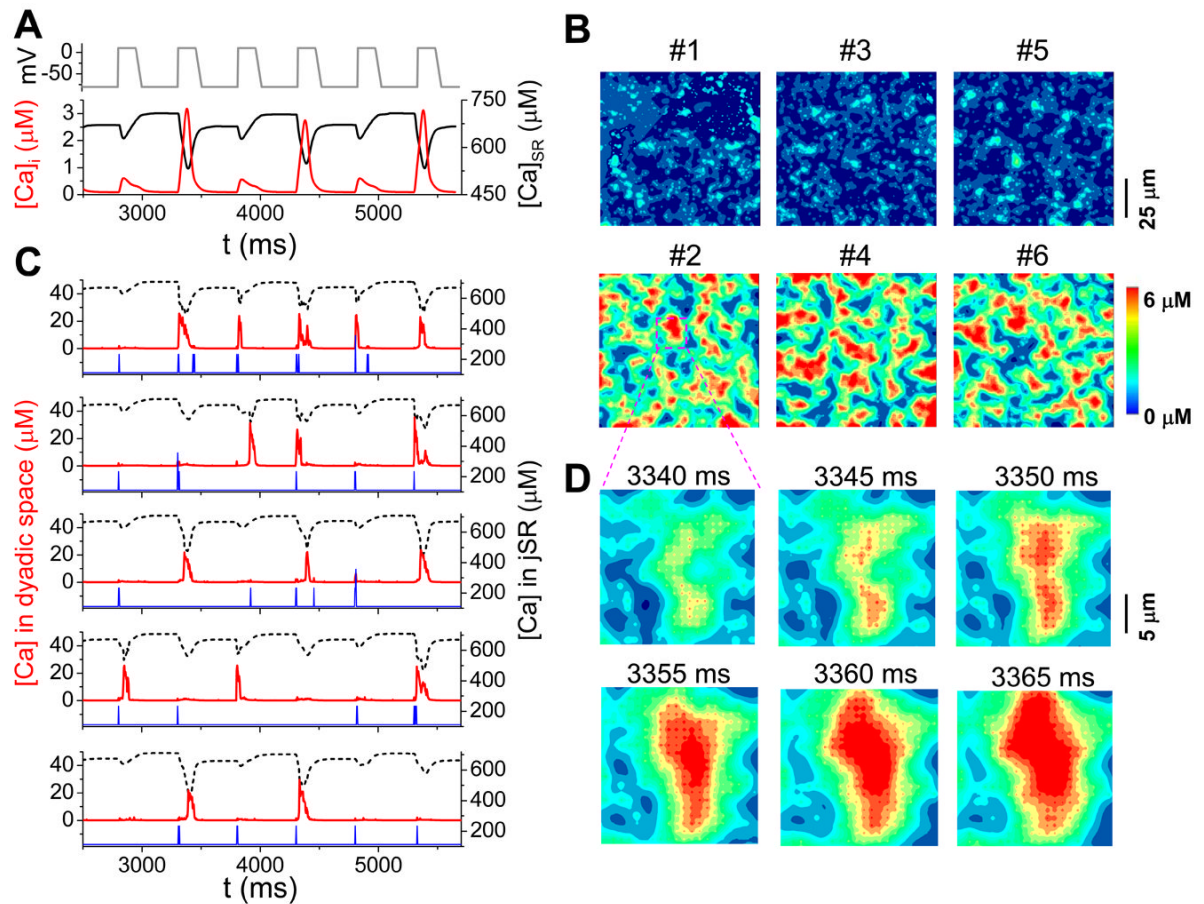
Figure 4. Ca alternans in the Ca cycling model
A. Clamped voltage (top), whole-cell SR Ca concentration (black), and whole-cell myoplasm
Ca concentration (red) versus time for PCL=500 ms. **B**. Ca traces from jSR (black dashed) and
dyadic space (red) at different spatial locations for the same simulation shown in A. The blue
line in each panel shows the Ca fluxes through the LCCs in the corresponding CRUs. **C**.
Snapshots of myoplasmic Ca spatial distribution taken at the moment of the Ca transient peaks
for the six consecutive beats shown in A. **D**. Ca snapshots from a small region (dashed box in
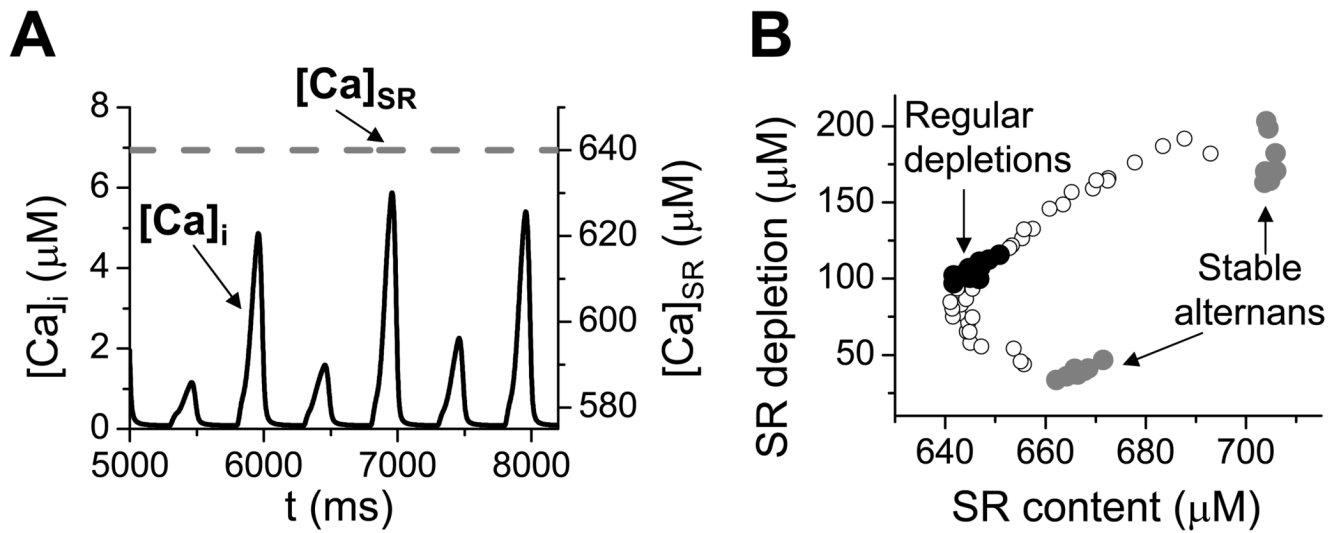beat #2 in panel C) show wave-like spread of Ca release.

Figure 5. Ca alternans does not rely on SR Ca load
A. Clamped SR Ca concentration (gray dashed) and myoplasmic Ca concentration versus time, PCL=500 ms. **B**. Ca depletion from SR versus SR Ca content as PCL increased gradually from 500 ms to 2000 ms in increments of 50 ms, with the initial 20 beats for PCL=500 ms ("stable alternans") and the last 10 beats for PCL=2000 ms ("regular depletion").
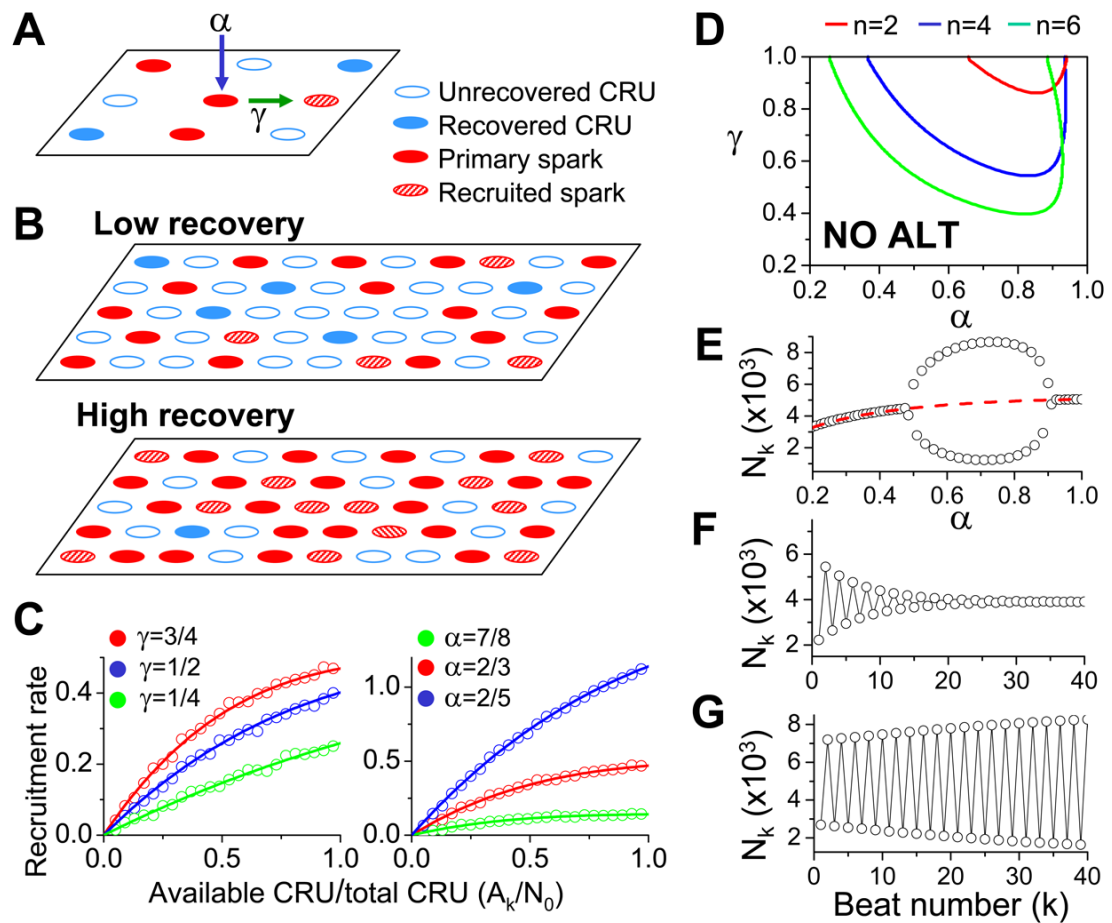
Figure 6. Mean-field theory of Ca alternans
A. Illustration of different CRU states and spark-induced sparks. α is the intrinsic probability an individual CRU will spark, while γ is the probability that one sparking CRU will recruit another to spark. **B**. Schematic plots illustrating recruitment rate at a low and a high recovery beat. C. Recruitment rate (defined as the ratio of recruited sparks to primary sparks) vs recovered ratio (defined as the ratio of available CRUs to total CRUs) for different γ when α=2/3 (left) and for different α when γ=0.75. Lines are theoretical results of Eq.4 which are confirmed by numerical simulations (symbols). Numerical simulations were done in a 100×100 CRU array, in which we first randomly assigned recovered and uncovered CRUs with a certain ratio, and then applied the rules outlined in A to determine the primary and recruited sparks. **D**. Phase diagram of α-γ parameter space for β=0.98 and different number (n) of neighbors, obtained analytically using Eqs.2 and 3 (see Online Supplemental Materials). **E**. Bifurcation diagram showing spark number vs. parameter α by iterating Eq.2 with γ=0.75 and β=0.98. For each α, the first 100 transient beats were dropped and the spark numbers in last 10 beats were plotted. **F** and **G**. Number of sparks versus the beat number from the non-alternating (α=0.5, γ=0.25, and n=4) and the alternating (α=0.8, γ=0.75, and n=4) regions in D.
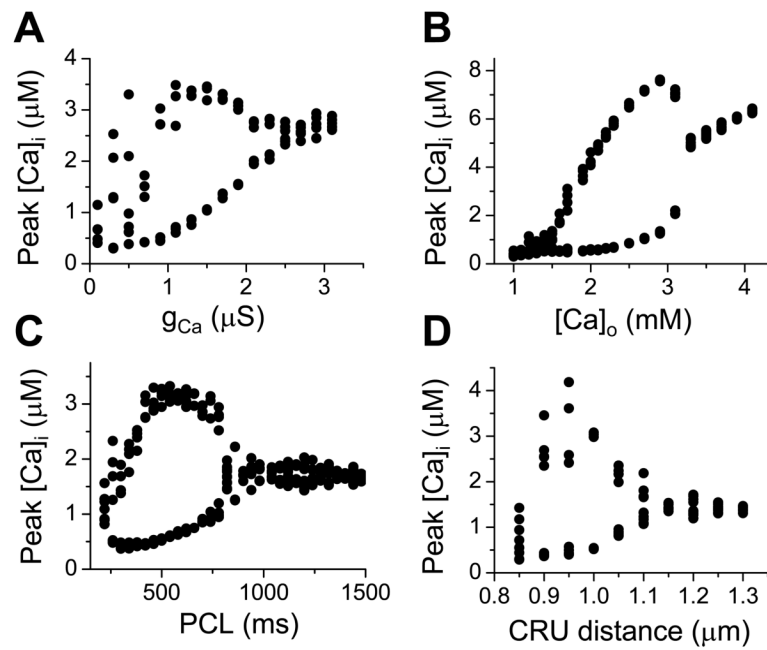
Figure 7. Predictions of the CRU network model of Ca cycling
A. Peak myoplasmic Ca concentration versus the maximum LCC conductance (g_{Ca}). **B**. Peak myoplasmic Ca concentration versus $[Ca]_o$. **C**. Peak myoplasmic Ca concentration versus PCL. **D**. Peak myoplasmic Ca versus CRU distance. In each panel, 5 to 10 peak myoplasmic Ca concentrations were plotted against each selected x-axis value.